Design of an Embedded Controller and Optimal Algorithm of PSA for a Novel Medical Oxygen Concentrator

Galang Adira Prayoga, Emir Husni, Salahudin Damar Jaya

School of Electrical Engineering and Informatics Institut Teknologi Bandung
Bandung, 40132 Indonesia
Corresponding author: Emir Husni (e-mail: ehusni@itb.ac.id).

Abstract: Oxygen therapy activities that are given to patients with respiratory problems (hypoxemia) and low oxygen saturation (SpO2) depend on the level of oxygen purity (O2%) of the additional oxygen supply. Getting supplemental oxygen can be easily obtained by patients in the market. There are several options to choose from, namely stationary and portable oxygen concentrator (Oxycon), which has a standard liter per minute (Lpm) of medical O2 (purity > 82%). The challenge in making Oxycon is making the device capable of producing pure oxygen stably and supplying flow oxygen to patients at a higher range (such as 5 to 80 Lpm) for special medical needs. Therefore, based on the problems faced and the existing challenges, the purpose of this study is to propose an embedded controller and optimize pressure swing adsorption (PSA) algorithm for a novel medical oxygen concentrator (MOC) by developing sub-system physics and hardware. The PSA method is applied to achieve this goal by assessing the appropriate cycle time according to Oxycon production capacity to produce pure oxygen as expected. Based on the studies that have been carried out, it is found that the appropriate time cycle for Oxycon with a capacity of 5 Lpm is 4000 milliseconds for the duration of adsorption in the zeolite tube. Testing at the MOC has been going on for the past two weeks, 12 hours a day. The sub-system physics, hardware, and software were successfully designed and implemented for the best MOC performance. Therefore, based on the study results obtained, the proposed algorithm and system are feasible to be implemented into a MOC system.

Index Terms: Medical Oxygen Concentrator; PSA; Algorithm of PSA; System Physics of MOC

1. Introduction

Currently, two types of oxygen concentrators in MOC can be found in the market: stationary and portable [1]. The main factors differentiating the two are the volume of oxygen produced, size and weight, power options, and price. Stationary oxygen concentrators have a higher volume of oxygen and require lower costs. Meanwhile, portable oxygen concentrators offer smaller sizes, lighter weights, and greater flexibility with battery resources. Stationary-type oxygen concentrators can produce about 0.5 to 10-15 Lpm of oxygen. As for the portable type, it can produce oxygen up to 2 Lpm [2][3][4].

Oxygen for industrial and medical applications is produced utilizing an oxygen concentrator. In the process of Oxygen Concentrator, several techniques can be applied: cryogenic distillation, PSA, and other approaches currently being developed. So far, the PSA method is the best for oxygen concentrators [1], It can be seen in Table 1. The working principle of PSA is to apply the focus of a typical compact adsorption-type oxygen concentrator which has two tube columns 15-30 cm long filled with Li-X zeolite particles with a diameter of 0.4-0.5 mm to separate oxygen from the air by implementing a process PSA [5]. Inside the adsorber tube column, nitrogen gas and its accompanying gas are adsorbed for a specific time so that oxygen from free air containing 78% nitrogen, 21% oxygen, 0.93% argon, and 0.038% carbon dioxide can be maximally concentrated. The high oxygen concentration separated in the adsorption column is transferred

Received: April 3th, 2023. Accepted: June 21th, 2023
DOI: 10.15676/ijeei.2023.15.2.4

to the oxygen tank and desorption column. Then nitrogen gas and its accompaniments are desorbed in another tube column or out through the exhaust pipe in the decompression process. The pressure and decompression operations change alternately to carry out the method according to a specified time cycle configuration depending on the oxygen production capacity. The concentration of oxygen released from the concentrator depends on the PSA's operational parameters and the zeolite column's characteristics. The discharge oxygen concentration depends on the volume, the temperature of the zeolite particles that fill the column, and the gas pressure and gas flow rate of the supplied air [5][6]. The PSA O2 production performance can be affected by the product flow rate as well as other process parameters, which are cross-correlated. For example, the product flow rate affects the purge flow rate, the adsorption pressure, and the feed flow rate, which associates with bed regeneration [6]. Table 1 presents a summary and a comparison of the oxygen storage mediums.

Table 1. Comparison of different oxygen storage mediums [7].

	Liquid Oxygen	PSA Plant	PSA Concentrator	Cylinders
Description	Liquid oxygen production off-site and stored in large tanks at the medical facility.	On-site oxygen generation using PSA technology.	A self-contained electrically powered medical device designed for the concentration of oxygen.	A refillable cylindrical storage and transportation of oxygen.
Electricity requirements	No	Yes	Yes	No
Maintenance requirement	Significant	Significant	Moderate	Limited
Distribution mechanism	Center pipeline distribution system	Central pipeline distribution system	Direct to patient areas	Direct to patient areas
Advantages	High oxygen output	Cost effective continuous supply of oxygen	Continuous oxygen supply that can be split among several patients	No power source
Disadvantages	Requires transport/supply chain. Need infrastructure. High maintenance for piping Requires cylinders as back up.	High capital investment Need infrastructure and uninterrupted power source. High maintenance for piping. Risk of leakage. Requires cylinders as back up.	Low pressure output. Requires uninterrupted power source. Requires cylinders as back up.	Requires transport/supply chain. Highly reliant on suppliers. Risk of leakage.

This study seeks to give a thorough analysis of the oxygen concentrator as a telemedicine tool for treating respiratory disorders from the system and software development standpoint to address the abovementioned issues. Our contribution to this study is to leverage PSA methods with optimization timing step cycle swing to produce pure oxygen ≥ 95%. The novelty of our proposed MOC is the system design and MOC algorithm whose zeolite adsorber performance can last for at least three months under high-humidity environmental conditions, such as in Bandung, Indonesia.

The study has been conducted by implementing an oxygen concentrator with a production capacity of 5Lpm. The remaining sections of this paper are organized to address the objectives of this research coherently. The related works and a novel oxygen concentrator discuss similar issues related to oxygen concentrators in section 2. In section 3, the algorithm of PSA for the oxygen concentrator is described. Section 4 addresses the results and discussion of MOC with a novelty design system MOC purposed. Section 5 concludes the study.

2. Relate Works

Research on oxygen concentrators using the PSA technique in its development has undergone many improvements in its performance in producing pure oxygen, more significant than 90%. A study conducted by Z. Qiao et al. [8] by applying the principle of pulse pressure-swing adsorption (PPSA) claims that the research contributes to a chosen particle size, bed length, and used pressure drop, there is an optimum combination of adsorption and desorption times that maximizes the product purity. The results suggest that there are operating windows for both 5A and partially Ag-exchanged Li-substituted 13X zeolite adsorbents where oxygen purity is greater than 90% in the product. In addition, in another study, S.W. Chai et al. [9] carried out a reduction of the bed size factor (BSF) of the PSA process with a value of 25-30 lbs/TPDc with an O2 recovery of 25-35% using: (1) Tiny particles of LiX zeolite (~0.35 mm), (2) Adsorption pressure of 3-4 atm, and (3) Total cycle times of 3-5 seconds. The research produces a 90-93% O2-enriched product gas from ambient air at a rate of 10 Lpm. Furthermore, the study [10] is conducting rapid pressure swing adsorption (RPSA) integrated with feedback control to operate MOC and also implemented a multivariable model predictive controller (MPC) for single bed MOC device. The single-bed proposed uses a four-step RPSA cycle that can be real-time controlled. However, the result of pure O2 production is in the range of 90%. Based on literature studies and experiments, the continuous production of pure oxygen with 95% purity stably at least 6 hours of daily use still needs to be done [22]. Because the high air humidity factor causes moisture saturation in the zeolite adsorber to accelerate, reducing the performance of zeolite in separating between N2, Ar, and O2 gases.

There are several alternatives to producing pure oxygen for medical needs, but not all are suitable for compact oxygen concentrator products. Table 2 compares the O2 production alternative methods based on the cost, efficiency, safety, energy utilization, pollutant emitted, market availability, and Oxygen purity level. Each method in the process of producing pure oxygen has its advantages. For example, the cost of getting the best pure oxygen by natural production (algae) was then ranked second with the PSA method. Regarding efficiency in getting pure oxygen, the PSA method is the best compared to others, and the second level is the membrane technology method.

Regarding safety for medical needs, the best way uses natural production (algae) and ranks second with the cryogenic separation method. Regarding the energy required to produce pure oxygen, the best approach is cryogenic separation which ranks second with the membrane technology method. Regarding the effect of pollutant emission on the environment, the best process is the membrane technology method, which ranks second with the PSA method. In the available market to obtain pure oxygen, the best approach with membrane technology ranked second with the PSA method. Regarding oxygen purity level, the best method with natural production (algae) ranked second with the cryogenic separation method and the worst way

among the three tracks with the PSA method. Therefore, research opportunities to increase oxygen purity levels stably in the PSA method are needed. If the oxygen purity level can be improved in the PSA performance method, therefore it can compensate for natural production and cryogenic separation methods, then the PSA method becomes a superior method in oxygen production.

Table 2. Ranking O_2 production based on the paper review [7].

	Natural Production (Algae)	Cryogenic Separation	Pressure Swing Adsorption	Membrane Technology
Costs	1 [11]	4 [12]	2 [13]	3
Efficiency	4 [14]	3	1 [15]	2
Safety	1 [11]	2 [13]	3 [13]	4 [13]
Energy Required	4 [16]	1 [17]	3 [13]	2
Pollutant Emission	4 [16]	3 [13]	2 [13]	1 [13]
Market Available	4	3	2 [18]	1 [19]
Oxygen Purity Level	1 [20]	2 [21]	4 [22]	3 [23]

3. System Architecture

The PSA system used is shown in Figure 1. The system consists of 3 valves (V1 to V3); the type of valve used is the directional control valve (KKA) 3/2, N/C. These valves' opened/closed status and the resulting flow resistance at each stage. Air is supplied to the column with a compressor, and then the air in the column is separated (into nitrogen and oxygen) by carrying out a four-stage PSA cycle. Stage 1 is the Initial air supply. Stage 2 is higher concentration oxygen transfer and gas discharge. Stage 3 is pressure equalization by transfer of higher concentration nitrogen. Stage 4 is air supply and gas discharge [24].

A pneumatic diagram in Figure 2 illustrates the working system on this MOC. The pneumatic system consists of 2 zeolite adsorber tubes, one oxygen collector tube, three valves, one compressor cooling fan (heat exchanger), one compressor, one pressure gauge, an oxygen sensor, pressure sensors, and HEPA filters. All components are assembled into one system, as depicted in Figure 2. In implementing this system, the type of zeolite used is the LiX molecular sieve type. The average diameter of the zeolite is (Dzeo) 0.48 mm. While the dimensions of the cylinder tube column (Dclm) are 65 mm, and the length (Lclm) is 160 mm. Inside the tube, there is a rectifier (Lrect) which contains silica gel with a size (Lrect) of 10 mm [5]. The PSA method is applied to the system.

In the PSA process, three valves are essential in regulating the opening/closing air circulation mechanism, and an orifice with a hole of 1 mm stabilizes the pressure balance between the tubes. In this PSA method, apply three stages. The first stage is the initial air supply. At this stage, the compressed air flowing from the compressor tends to increase in temperature. The radiator then helps heat air cooling.

Furthermore, the air is supplied to one of the tubes through the mechanism of opening valve tube one and closing valve tube two until it reaches an absolute pressure of 250 kPa. The second stage is the condition of higher concentration oxygen transfer and gas discharge. At this stage, valve three will open, and oxygen will flow into tube 3. The third stage is the process of pressure equalization by transfer of higher concentration nitrogen. A close valve tube one mechanism and an open valve pre-charge mechanism are applied at this stage. Therefore, by closing valve tube

1, the higher concentration of nitrogen will come out of tube 1 through the exhaust mufflers, and with open valve pre-charge, the pressure between the tubes is equalized. The 3-step mechanism works alternately on each tube and produces concentrated oxygen ≥ 95%.

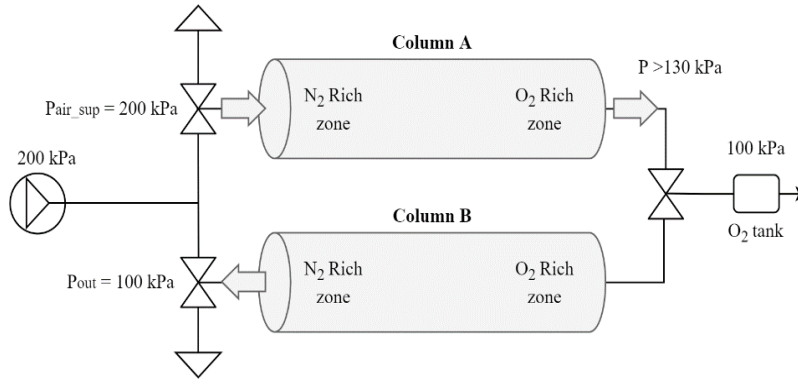

Figure 1. Schematic of the PSA system and gas flow in PSA cycle

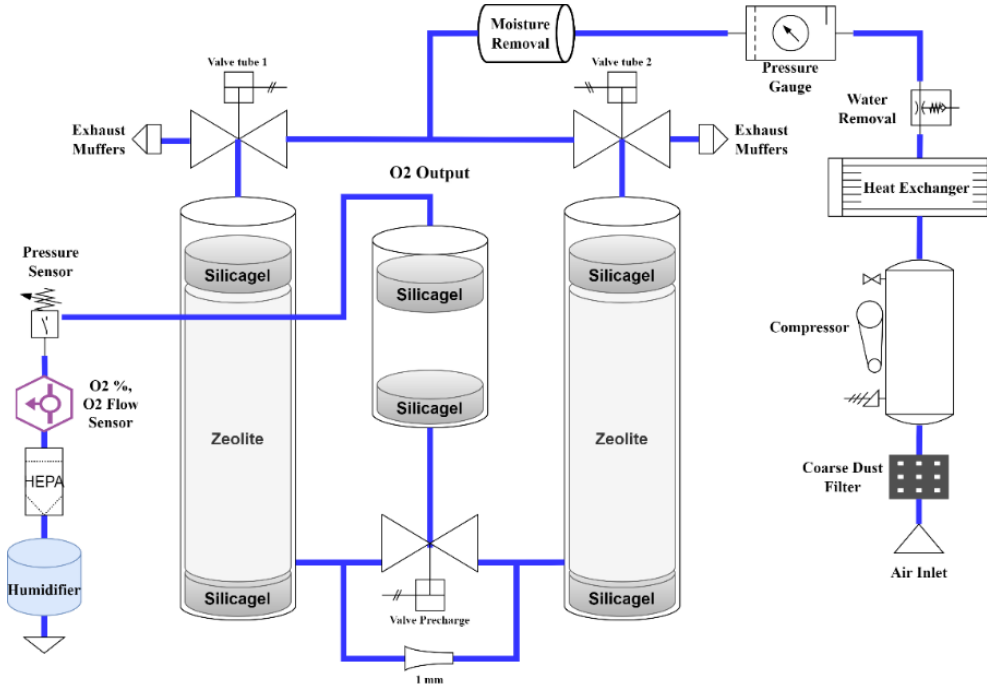

Figure 2. Architecture of Sub-System Physics MOC

The hardware of this system consists of several sensors and actuators integrated by a microcontroller. A PCB Board is made to facilitate installation between sensors and other supporting components. The PCB board will contain each pin of each sensor, such as the oxygen concentrator sensor (OCS) to measure oxygen gas, pressure sensor, alarm, indicator lamp, and valve, which functions as a control unit and data acquisition, where the data from the sensor readings will be processed by the microcontroller before being sent to the ESP module as a Wi-Fi module and display the data to LCD. The data obtained by the ESP module from the microcontroller is then sent to the database by wireless communication. The data that is collected

into the database every 3 seconds is in the form of O2%, O2 flow, O2 Temperature, O2 Pressure, Oxycon Time Operation, and device id data (Figure 3). Data collection every 3 seconds aims to get time series data that is useful for the needs of prediction systems in the future. In addition, with every 3-second delivery to avoid data loss when transferring [25]. But it depends on the need. If you have a good internet bandwidth and a slight latency, the lag time can be shortened so that the time-series data is better.

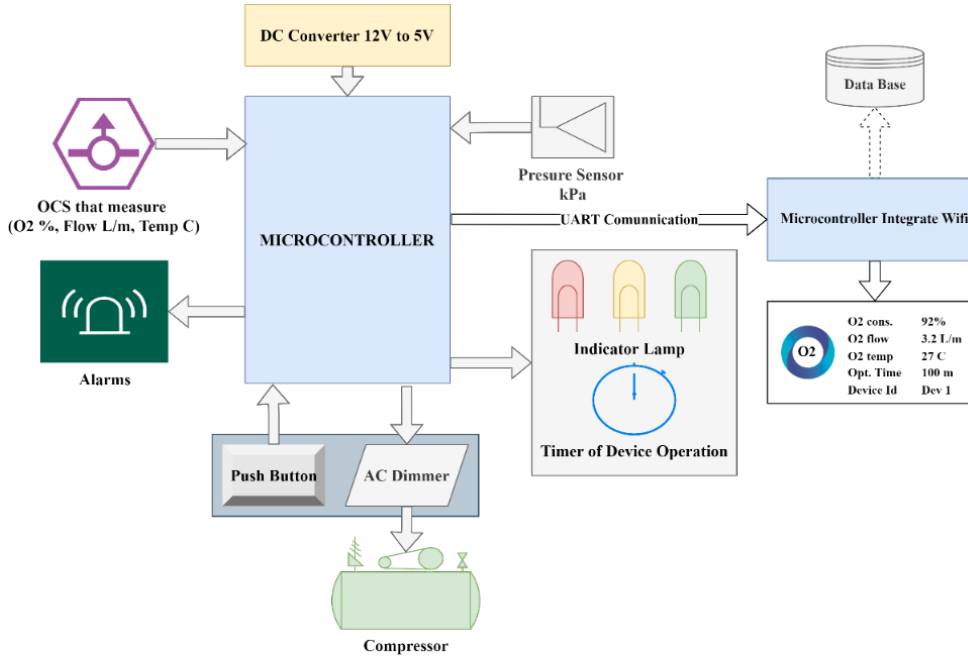

Figure 3. Architecture of Electromechanical MOC

4. Device Design

A. Sub-system Physics Analysis and Design Prototype of Oxygen Concentrator Mobile

In this research, the development model was carried out using the throwaway prototyping model [26] to obtain the expected MOC product analysis and design. The system is designed by considering the temperature and humidity factors of the air supplied to the zeolite sieve adsorber tube. It is known that the humidity in tropical countries like Indonesia, especially at an altitude of 900 meters above sea level, has an average humidity of 70% [27] and an ambient temperature of 29 ℃ [28]. High air humidity can reduce the performance of zeolite sieves in filtering nitrogen gas (N_2) [29]. Therefore, to get low-humidity air, it is necessary to do treatment water removal and moisture removal on the MOC system. The water removal process begins by applying air condensation to the radiator. The compressed air from the compressor pump has a temperature of about 40 ℃ with high humidity. Therefore, by passing air through the radiator grille with air conditioning relying on air circulation around 28 ℃, the air with high moisture condenses and becomes water droplets carried by the compressed air. Water droplets flowing with the compressed air will be trapped through water removal so that the air passed on is dry without water content. However, the flowing dry air must lower its humidity level again through a tube containing alumina silica gel. Therefore, the air that will be channeled into the zeolite sieve tube is low-humidity air. An illustration of the MOC design system can be seen in Figure 4.

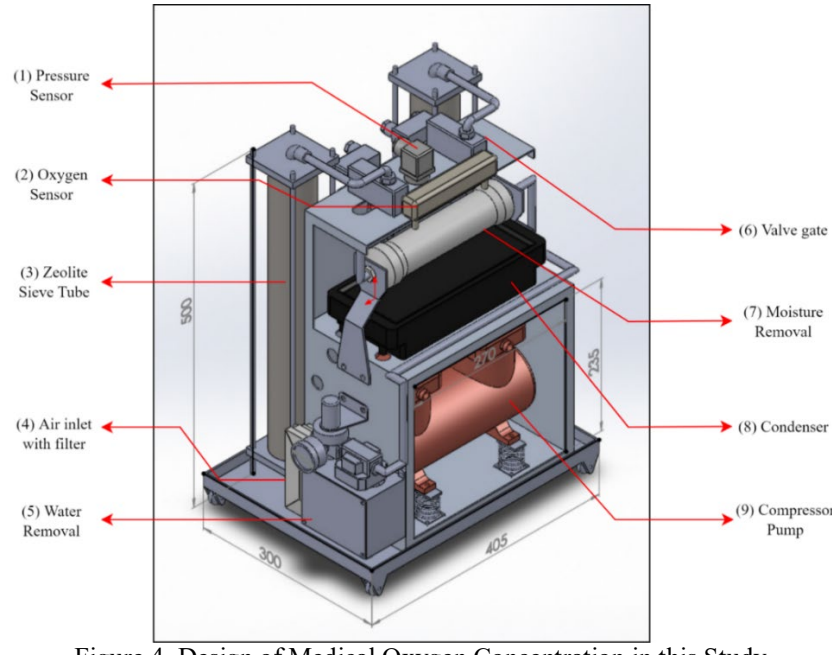

Figure 4. Design of Medical Oxygen Concentration in this Study

Air with low humidity that will be forwarded to the zeolite sieve adsorber tube has a pressure of 150-200 kPa. The zeolite sieve will filter the environment, which consists of oxygen (O2), nitrogen (N2), argon (Ar), and other ancillary particles [30]. O2 gas will be allowed to pass through the filter, and N2, Ar, and other accompanying particulate gases will be retained by the zeolite sieve during the pressurization and adsorption (PR & AD) process. The gas N2, Ar, and other accompanying particulates will then be discharged back into the ambient air during the purge process (PG). In this process, the size factor of the tube/bed adsorber zeolite sieve is an important thing that must be analyzed to obtain stable 95% pure O2 results. For the needs of MOC with a production capacity of 5 Lpm, the design and dimensions of the zeolite sieve tube are obtained as shown in Figure 5. The dimensions of the tube are 440 mm in height, 58 mm in diameter, 2640 mm^2 in cross-sectional area, and 1,161 cm^2 in volume. Then inside the tube on the top and bottom sides, there is a membrane separator to filter so that the particulates contained in the zeolite sieve are not carried away during the pressurization and adsorption (PR & AD) and purge (PG) processes. On the top tube cover where the compressed air will be supplied, there is a spring to provide a compressive force so that the zeolite sieve is solid without leaving space so that the filtration process is maximized.

Based on the equilibrium adsorption theory (see Figure 5), each gas component will feel pressure with the compressive force. F is the compressive force of air exerted in the N2 and Ar gas filtration process and the O2 gas release process for a certain duration of time (Δt) and in tubes along L and Cross-sectional area A. The amount of gas N_2, Ar, and O_2 is represented by N as the number of particles (Avogadro number). The gas pressure force N_2 equation in the adsorption process is written by equation (1). Then the gas pressure force equation O_2 in the adsorption process is written with equation (2). The equation of force of gas pressure Ar in the adsorption process at the initial stage is written with equation (3). Finally, the pressure force of gas Ar at the end of the adsorption column is equivalent to zero written by equation (4).

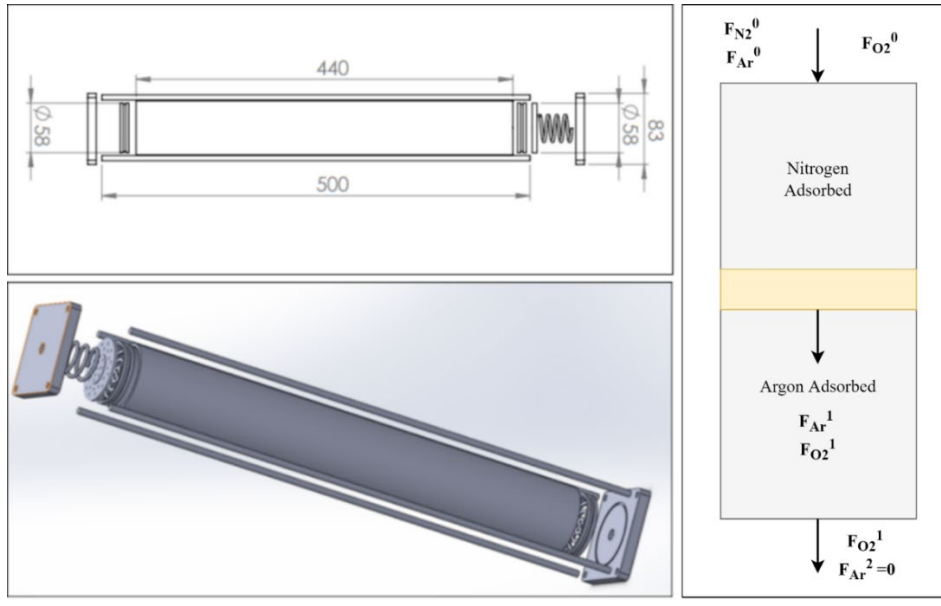

Figure 5. Design of Adsorber Tube Medical Oxygen Concentration

$$\text{Nitrogen} \rightarrow F_{N2}^0 \Delta t = \Delta L_1 A N_{N2}^1 = v_1 A N_{N2}^1 \quad (1)$$

$$\text{Oxygen} \rightarrow F_{O2}^1 = F_{O2}^0 + (N_{O2}^2 - N_{O2}^1) A v_1 \quad (2)$$

$$\text{Argon} \rightarrow F_{Ar}^1 = F_{Ar}^0 + (N_{Ar}^2 - N_{Ar}^1) A v_1 \quad (3)$$

$$\text{Argon} \rightarrow F_{Ar}^2 = 0 = F_{Ar}^1 + N_{Ar}^2 A v_2 \quad (4)$$

For the adsorption bed to remove both nitrogen and argon the velocity ratio of the argon front must be greater than that of the nitrogen front. Therefore, the equation (5) can be written as:

$$\frac{v_2}{v_1} = \frac{\frac{F_{Ar}^0}{F_{N2}^0} + (N_{Ar}^2 - N_{Ar}^1)}{N_{Ar}^2} > 1 \quad (5)$$

The suggested MOC pressure stabilizer system controls the pressure between two zeolite sieve tubes to maintain stability. O_2 gas which will go through the blow down process to the O_2 collecting tube occurs with a certain time lag, therefore the pressure in one of the tubes will be higher as shown in the blue arrow line in Figure 6. This higher pressure occurs due to the effects of the pressurization and adsorption (PR & AD) processes in the tube. Therefore, the ability to produce 95% pure O_2 depends on a pressure stabilizer's presence. The pressure stabilizer must also fulfill as described in equation (5) before.

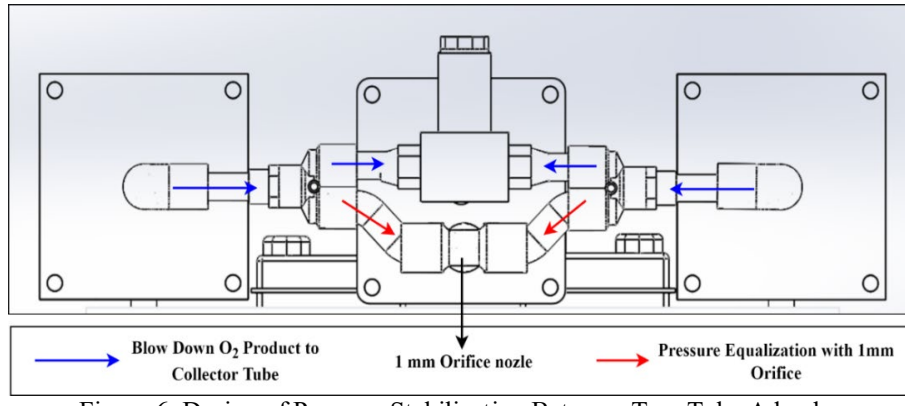

Figure 6. Design of Pressure Stabilization Between Two Tube Adsorber

As seen in Figure 7 below, the implementation of the results of the design and analysis of the MOC system is carried out by developing throwaway prototyping. Figure 7. (a) the overall system form of the MOC without the enclosure installed. Figure 7. (b) is a compressor pump component that takes in air with the ability to supply air flow rate ≥ 75 Lpm with a pressure of 200 kPa and power consumption ≤ 320 W. Figure 7. (c) a radiator component to cool compressed air and condense so that air and water can separate. Figure 7. (d) a water removal component to separate the compressed air from the carried water vapor particles so that only compressed dry air will be forwarded. Figure 7. (e) an alumina-silica gel tube to reduce air humidity after passing through water removal. Therefore, the air that will be passed by is dry. Figure 7. (f) two zeolite sieve tubes for carrying out the PSA process and one oxygen collection tube.

B. Hardware Design

The electrical path for the PSA control system, sensors, and several indicators is connected to the microcontroller I/O pin (Figure 8). In the circuit design, a 12-VDC direct current (DC) voltage drop to 5-VDC is applied for the microcontroller input voltage. Meanwhile, the servo valve module, oxygen sensor, and pressure sensor require a 12-VDC voltage.

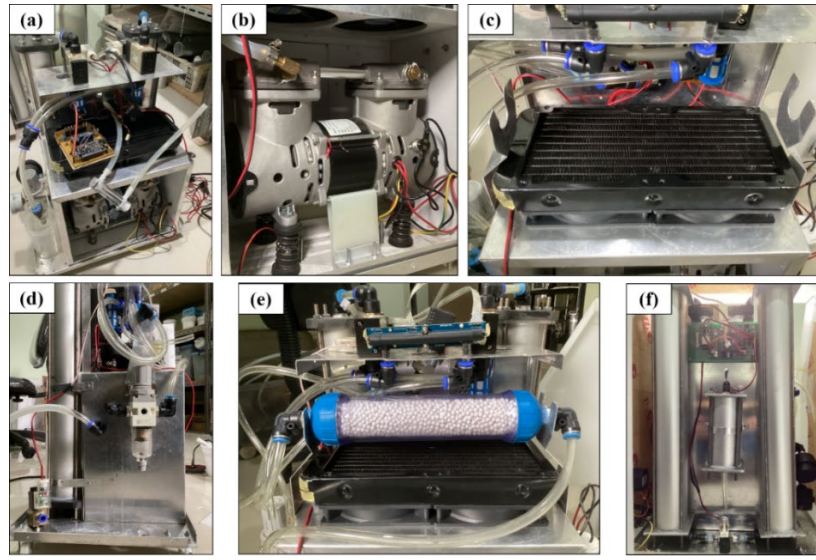

Figure 7. Implementation of Sub-System Analysis for MOC

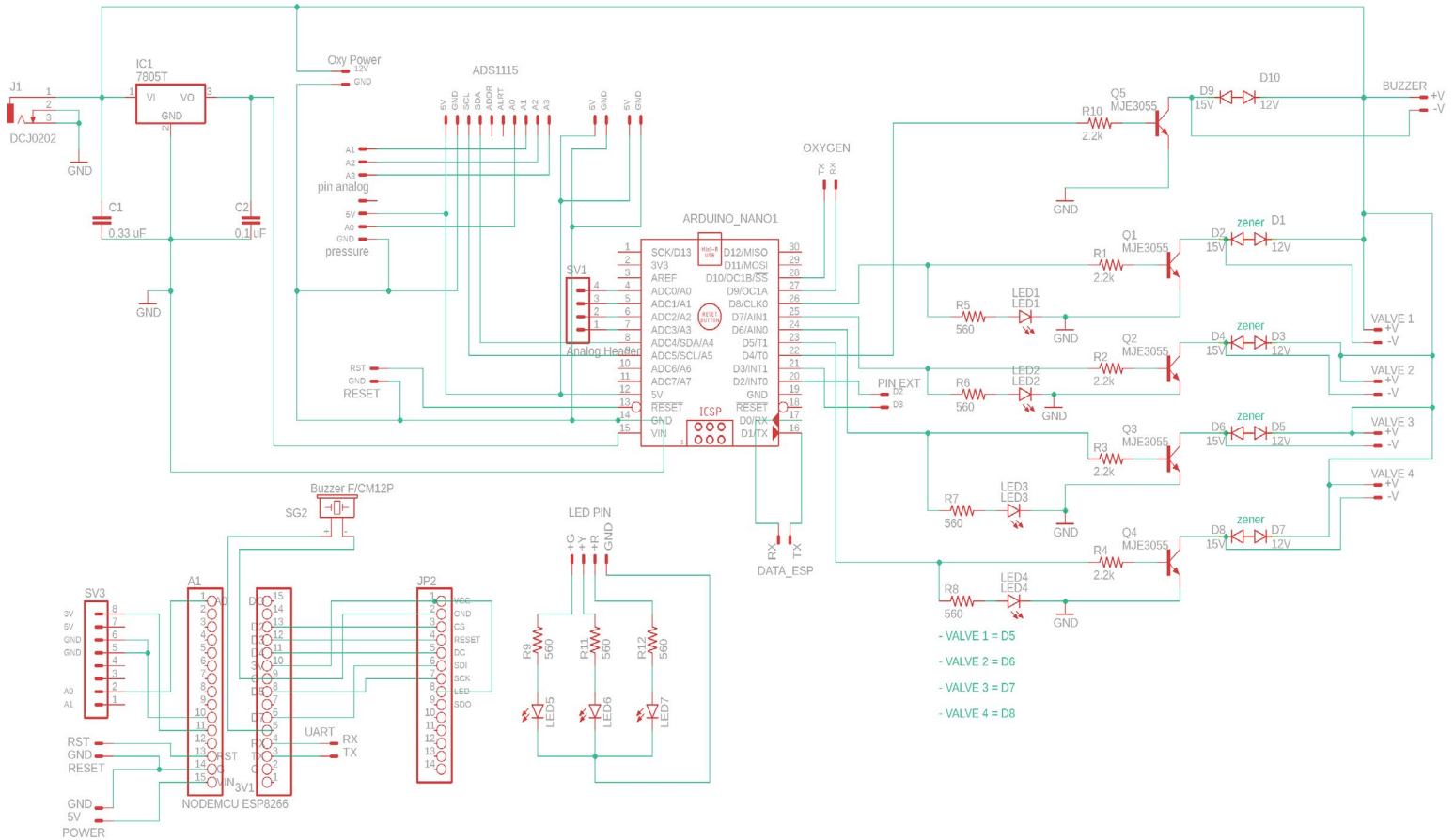

Figure 8. Sequence Design of MOC Controller

The design of an embedded system on an oxygen concentrator controller capable of telemetry communication is controlled by two microcontrollers. The first microcontroller (M-1) was a microcontroller with 8-bit processor specifications, 16 MHz clock frequency, 32 kB bootloader, 2 kb internal SRAM, 1 kb EEPROM, and serial communications such as UART, SPI, and I2C. Meanwhile, the second microcontroller (M-2) is a microcontroller system on chip (SoC) with 32-bit processor specifications, 448 kB ROM, 520 kB SRAM, 40 MHz Wi-Fi/Bluetooth, Wi-Fi 802.11n (2.4GHz), 8 MHz internal oscillator, 8-bit digital to analog converter, and serial communications such as SPI, I2S, I2C, and UART. The M-1 controls the PSA system and monitors the output of O2 and its pressure. At the same time, the M-2 functions as a wireless communication to remotely monitor the device via an internet connection (See Figure 9).

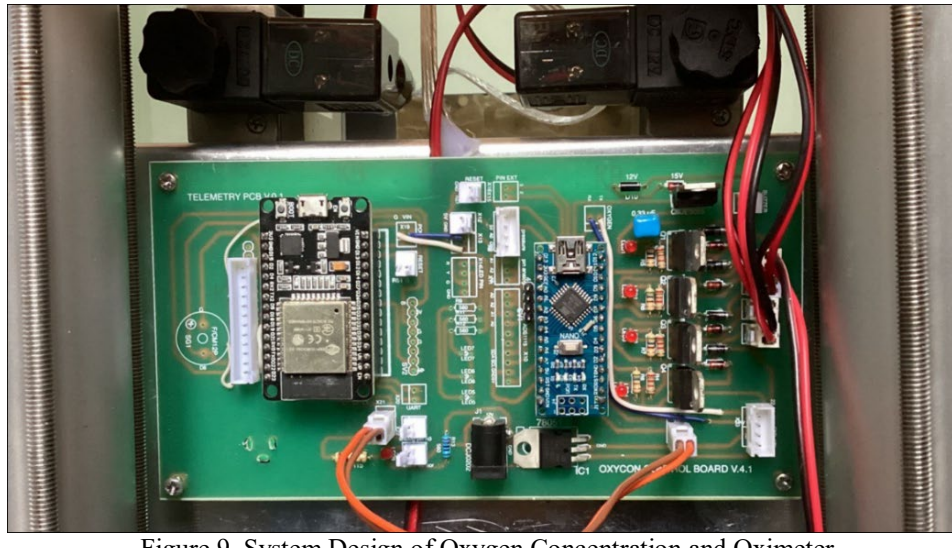

Figure 9. System Design of Oxygen Concentration and Oximeter Integrated IoT System Mobile

The switch uses an npn type of transistor component with the manufacturer's code TIP120/TIP121/TIP122. The technical specifications of such transistors depend on the manufacturer's code. For example, Collector-Emitter Sustaining Voltage for TIP120 (60 V), TIP 121 (80 V), and TIP122 (100 V). In the embedded design, we use the manufacturer's code TIP 121. The Collector-Emitter Saturation Voltage transistor specifications are $V_{CE(sat)}$ = 2.0 V (Max) and the collector current (I_C) = 3.0 A. Then the base current (I_B) is 120 mA [31]. The architecture of the transistor circuit is shown in Figure 10.a.

Theoretically, activating a transistor as a switch entails doing so at one of the saturation or plug points but not along the load line. A transistor is like a closed switch from collector to emitter when saturated [32]. The transistor is similar to an open switch if it is turned off/cut off. Figure 10.b shows a closed-loop circuit as a flowing current analysis model. Where the sum of the voltages around the loop gives the equation (6):

$$I_B R_B + V_{BE} - V_{BB} = 0 \quad (6)$$

By solving I_B, we get the equation (7):

$$I_B = \frac{V_{BB} - V_{BE}}{R_B} \quad (7)$$

For example, V_{BB} = 5 V and R_B = 2,2 kΩ. Then:

$$I_B = \frac{5\,V - 0{,}7\,V}{2{,}2\ \text{k}\Omega.} = \frac{4{,}3\,V}{2{,}2\ \text{k}\Omega.} = 1{,}9\,mA$$

The transistor looks like a closed switch if the current is greater than or equal to $I_{B(sat)}$. Conversely, if the base current is zero, the transistor looks like an open switch. It means that if the switch is open, then the electrons from the collector to the emitter are equal to 0.

Figure 10.c shows a switch circuit design for controlling a valve represented by an LED. This circuit is called a valve driver because the transistor controls the valves. If the input voltage is low, the transistor will be cut off, and the valve will not turn on. If the input voltage is high, the transistor is in saturation, and the valve is on.

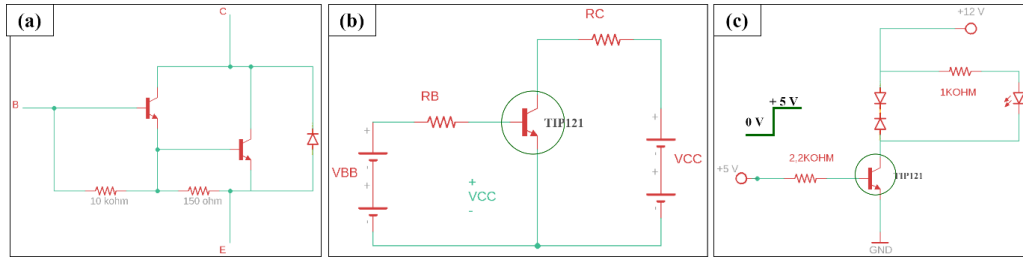

Figure 10. Using Transistor as Switches (a) architecture TIP121, (b) close loop switch, and (c) implementation for valve switch

5. Performance Calculation and Algorithm of The PSA System

A. Performance Calculations

Oxygen production, assessed using the PSA method, is influenced by factors such as air humidity, air temperature, zeolite quality, nitrogen uptake rate by zeolite, etc. Based on the ideal gas law equation, it is assumed that the oxygen and nitrogen behaved can be explained by equation (8) and moles of gas are obtained by equation (9):

$$P_s \Delta V_{cv,gas} = n_{gas,s} R_{gas,s} T_{gas} \quad (8)$$

$$n_{gas,s} = \frac{R_{gas,s} T_{gas}}{P_s \Delta V_{cv,gas}} \quad (9)$$

Where P_s is the partial pressure of gas in a column, $\Delta V_{cv,gas}$ is the void volume of a control volume (as a differential volume element which divides the column into thin disk shapes the product of the void area of the cross-section of a column, $A_{cv,gas}$ and the length of the control volume, ΔL_{cv}), $n_{gas,s}$ is the mass of gas in the control volume, $R_{gas,s}$ is the gas constant, T_{gas} is the gas temperature in the control volume. The subscirpt, s, denotes the gas species (O_2 or N_2) [5]. To maximize the gas, both Oxygen ($n_{gas,O2}$) released and Nitrogen ($n_{gas,N2}$) adsorbed, equation 2 is required. Then, by understanding that the mass of gas adsorbed by the zeolite ($m_{abs,s,eq}$) is affected by the mass of the zeolite (m_{zeo}), isothermal capacitance in mass units (Q_s), and Langmuir constant (K_s). Therefore, the equation (10) can be written as follows:

$$m_{abs,s,eq} = \frac{m_{zeo} Q_s K_s P_s}{1 + \sum_s K_s P_s} \quad (10)$$

When the gas flows through the zeolite with a specific flow rate, the mass conservation equation (11) for the gas in volume control is expressed as follows.

$$\frac{\partial}{\partial t}\left(\frac{P_t}{T_{gas}}\right)+\frac{\partial}{\partial x}\left(\frac{uP_t}{T_{gas}}\right)=\frac{\partial}{\partial x}\left\{D_{eff,ax}\frac{\partial}{\partial x}\left(\frac{P_t}{T_{gas}}\right)\right\}-\frac{1}{\Delta V_{cv,gas}}\sum_s\left(R_{gas,s}\frac{\partial m_{abs,s}}{\partial t}\right) \quad (11)$$

Where u is the gas flow velocity through the zeolite as a porous medium; P_t is the conservation equation of total gas pressure; $D_{eff,ax}$ is the effective diffusion coefficient of gas flowing in the packed bed in the axial direction.

The implemented system assumes that the spatial distribution of total gas pressure is uniform within the zeolite column. Therefore, the partial differential with the following equation (12):

$$\frac{\partial P_t}{\partial x}=0 \quad (12)$$

If the partial differential is applied to equation (11) and substituting equation (12), the time parameter will be obtained as a reference in the gas adsorption process with equation (13).

$$\frac{1}{\hat{T}_{gas}}\frac{\partial P_t}{\partial t}-\frac{P_t}{\hat{T}^2{}_{gas}}\frac{\partial T_{gas}}{\partial t}+P_t\frac{\partial}{\partial x}\left(\frac{u}{T_{gas}}\right)=-\frac{\partial}{\partial x}\left\{D_{eff,ax}\frac{P_t}{\bar{T}^2{}_{gas}}\frac{\partial T_{gas}}{\partial x}\right\}-\frac{1}{\Delta V_{cv,gas}} \quad (13)$$

Where $\hat{T}_{gas}$ is the time average gas temperature between t and $(t+\Delta t)$, $\bar{T}^2{}_{gas}$ is the spatial average gas temperature, and Δt is the time step in the numerical simulation [5].
For the O_2 purity (%) is calculated from the following equation (14):

$$O_2\ purity=\frac{\int_0^t y(t)p(t)dt}{\int_0^t p(t)dt} \quad (14)$$

Where $y(t)$ and $p(t)$ are the volume fraction of O_2 in product and instantaneous product flow rate, respectively [6].

B. Algorithm of PSA System and Cycle Description

The concentrated oxygen production process using the Pressure Swing Adsorption (PSA) method requires a control system to set the timer for each stage, such as the pressure/Pressurization (PR) time given to the adsorber tube, gas adsorption (AD) time, gas release time from the adsorber tube. To the collection tube/Blow Down (BD), nitrogen-rich air purge time/Purge (PG), and pressure equalization/Equalization (EQ) time. The cycle time configuration dramatically affects the stability in producing concentrated oxygen ≥ 95%. Therefore, looking for the appropriate control system algorithm can achieve the objectives of the oxygen concentrator. Based on several research articles published in the upper quartile (Q1), many algorithms are offered, such as research conducted by [10] proposing a scheme with four timing stages. Research conducted by [6] suggests a scheme with eight timing stages. However, from the two studies referred to as the primary reference, the research schemes were carried out under different conditions. Urich et al. conducted research by implementing an adsorber tube with an adaptive controller and a predictive system controlled by the Raspberry Pi microprocessor. While Zhang et al. conducted research by implementing two tubes with a responsive control system.

Based on the corresponding problem, to realize a mobile oxygen concentrator product capable of producing 95% stable pure oxygen. The algorithm applied to the PSA system is a responsive control system algorithm with six timing stages (see Figure 11) and is equipped with a pressure stabilizer in the form of an orifice with a diameter of 1 mm as a substitute for the rapid

and incomplete depressurizing pressure equalization (RIDPE) process proposed by the research of Zhang et al. The six timing stages in the proposed algorithm are pressurization and adsorption (PR & AD), blow down (BD), blow down and equalization (BD & EQ), purge (PG), equalization (EQ), and pressurization (PR). Step 1 occurs the PR & AD process in tube 1 and PG in tube 2. Step 2 occurs the BD process in tube 1 and the EQ process in tube 2. Step 3 occurs the BD & EQ process in tube 1 and the PR process. Step 4 occurs the PG process in tube 1 and the PR & AD process in tube 2. Step 5 occurs the EQ process in tube 1 and the BD process in tube 2. Step 6 occurs the PR process in tube 1 and the BD &; EQ process in tube 2.

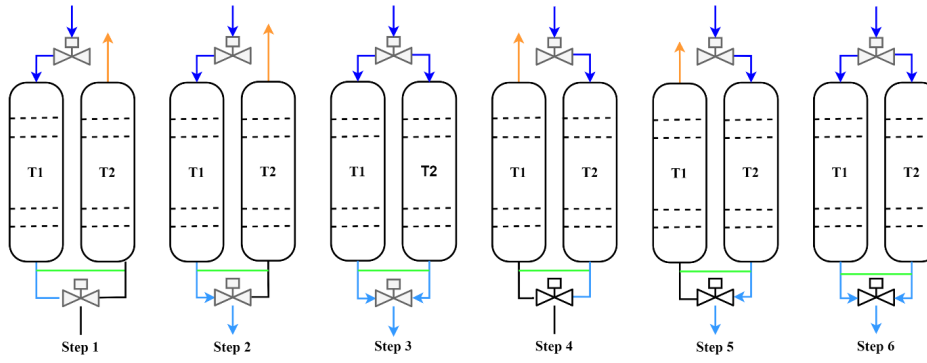

Item	Step 1	Step 2	Step 3	Step 4	Step 5	Step 6
Duration	4000 ms	350 ms	650 ms	4000 ms	350 ms	650 ms
T1	PR & AD	BD	BD & EQ	PG	EQ	PR
T2	PG	EQ	PR	PR & AD	BD	BD & EQ

Figure 11. Algorithm Scheme of PSA control in Oxygen Concentrator

Considering the dimensional factors and the size of the zeolite sieve adsorber tube, determining the timer for each stage, as shown in Figure 11, requires theoretical calculations to maintain the service life of the zeolite sieve. But technically, to get the optimal timer to be applied to the PSA system cycle, a process of repetition and iteration is carried out; therefore, that the appropriate time is obtained. However, before carrying out the iteration, it is necessary to know the lower limit value of the timer for the pressurization and adsorption process so that it can speed up the search process. In the PSA design that implements two adsorber tubes, each adsorber tube timer stage will work according to its duties, as shown in Figure 11. When the PSA system is started by configuring the timer function u[k], which is the total time of each specified timer stage as shown in Figure 12, it will be known whether the resulting oxygen production has reached the expected value or not. If the predetermined timer configuration does not find the appropriate pure oxygen production results, it will add time n+1000, where n starts from 0 to 10,000 in milliseconds.

6. Result and Discussion

In the process of adsorption of N2 gas carried out by zeolite sieve, the parameters of the air pressure supplied from the compressor greatly affect the ability of Oxycon to produce pure oxygen ≥ 95%. Oxycon, with a production capacity of 5 Lpm requires a minimum air pressure supply of 150kPa from the compressor to the zeolite tube. However, what must also be considered is the length of time the air pressure is applied to the zeolite sieve tube. If this time exceeds the saturation limit of gas adsorption carried out by the zeolite sieve, then the production of pure oxygen will not be optimal. As shown in Table 3, finding the optimal time to cycle each

tube of zeolite is the key to producing ≥ 95% oxygen. The term of the valve control signal to regulate the compressed air flow path is shown in Figure 13. Where V1 is Valve 1, which is connected to the zeolite sieve tube 1 (T1) at the compressed air intake (top of the tube), V2 is Valve 2 which is connected to the zeolite tube sieve 2 (T2) at the compressed air intake (top of the tube), and V3 is valve 3 which connects T1 and T2 at the end of the tube (bottom of the tube) which is the result of gas filtration which produces pure O2 and flows pure O2 to the collector tube. Then in Fig. 13, the tendency for pure oxygen will decrease if the flow of oxygen delivered to the patient is higher. To be able to overcome this is to engineer the size of the Orifice nozzle hole. In his implementation, the optimal Orifice with a hole size of 1mm for a production capacity of 5 Lpm.

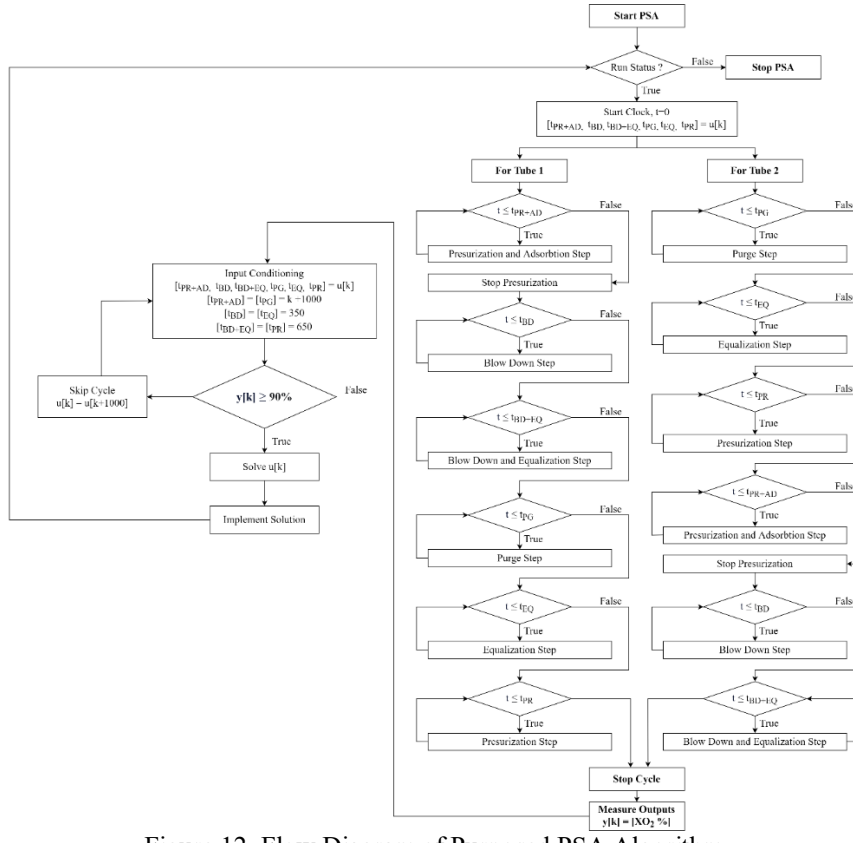

Figure 12. Flow Diagram of Purposed PSA Algorithm.

Table 3. Cycle-time testing for stable pure oxygen production.

Item		Step1	Step2	Step3	Step4	Step5	Step6
T1		PR & AD	BD	BD & EQ	PG	EQ	PR
T2		PG	EQ	PR	PR & AD	BD	BD & EQ
Duration (ms)	S1	3000	350	650	3000	350	650
	S2	4000	350	650	4000	350	650
	S3	5000	350	650	5000	350	650
	S4	6000	350	650	6000	350	650
	S5	7000	350	650	7000	350	650
	S6	8000	350	650	8000	350	650
	S7	9000	350	650	9000	350	650

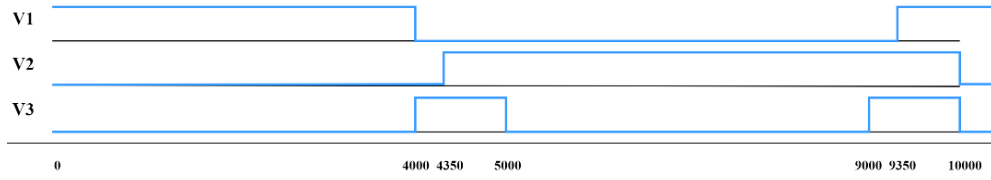

Item	Step 1	Step 2	Step 3	Step 4	Step 5	Step 6
Duration (ms)	0-4000 ms	4000-4350	4350-5000	5000-9000	9000-9350	9350-10000
V1	HIGH	HIGH	HIGH	LOW	LOW	HIGH
V2	LOW	LOW	HIGH	HIGH	HIGH	HIGH
V2	LOW	HIGH	HIGH	LOW	HIGH	HIGH

Figure 13. Time Step for Signaling the Valve Open/close Gate.

A. Optimum Cycle Tine Performance

The results of oxygen concentrator production testing have been obtained in the form of oxygen production data with an output oxygen flow of 5 Lpm based on testing the variation of the PSA system cycle time. The experiments that have been carried out aim to get the best cycle time in the adsorption process carried out by the zeolite. In the time search process for each stage, the best cycle time obtained for a 5 Lpm oxygen concentrator production capacity is time cycle 2 (S2). Time cycle 2 (S2) has a time duration of Pressurization and Adsorption (PR & AD) of 4000 milliseconds, blow down (BD) of 350 milliseconds, blow down and equalization (BD & EQ) of 650 milliseconds, purge (PG) 4000 milliseconds, equalization (EQ) 350 milliseconds, and pressurization (PR) 650 milliseconds (See Figure 14).

Based on figure 14 shows the results of oxygen production with variations in the timer cycle carried out by the search process with the grid search method. Cycle 2 (S2) with a duration of 4000 ms PR & AD process (step 1) in tube 1 and a duration of 4000 ms PG process (step 4), the process is carried out alternately regularly as in Figure 13, giving the best results with 95% oxygen production stably for an oxygen production capacity of 5 Lpm. Cycle 1 (S1) gives a good oxygen production result but not a maximum of 95%. Cycle 3 (S3) in the first minute of the production process was quite good, but after a while, production dropped and stabilized at a value of 85%. Cycle 4 (S4), cycle 5 (S5), cycle 6 (S6), and cycle 7 (S7) result in unstable oxygen production and oscillating causes in oxygen production.

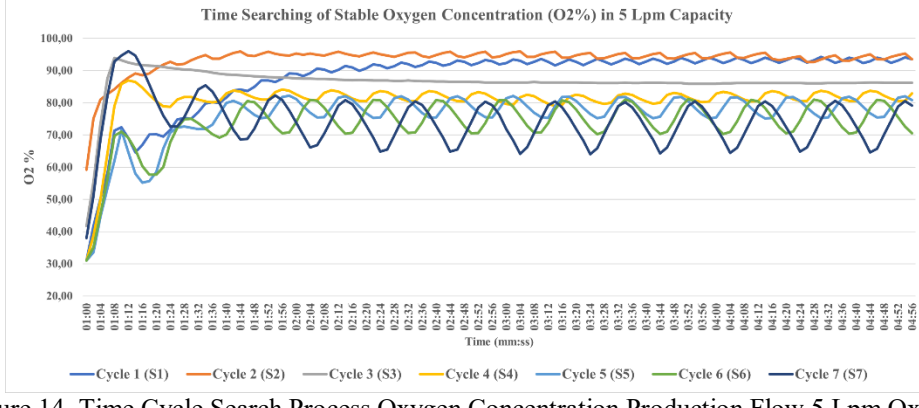

Figure 14. Time Cycle Search Process Oxygen Concentration Production Flow 5 Lpm Oxygen (%) Based on Grid Search.

B. O_2 Production Performance

System testing has been done with a throwaway prototyping development system for one month. Design, implementation, and assessment are used concurrently in the development procedure to get the best performance out of the oxygen concentrator. Therefore, the objective of developing an oxygen concentrator device may be adequately accomplished, more evaluation will be conducted to obtain a completely tested product design. Throughout the test, a stable 95% pure oxygen production was attained. As depicted in Figure 15, the test was run six hours daily. By testing the application of the orifice, with a variation of the nozzle hole of 1 mm, 1.5 mm, and 2 mm, it was obtained that the orifice nozzle hole was suitable for an oxygen production capacity of 5 Lpm by applying 1 mm. The pressure generated in the production oxygen collection tube is in the range of 80-90 kPa for a flow range of 4-5 Lpm (see Figure 16). The higher the flow of oxygen given to the patient, the lower the pressure in the oxygen collection tube produced will be.

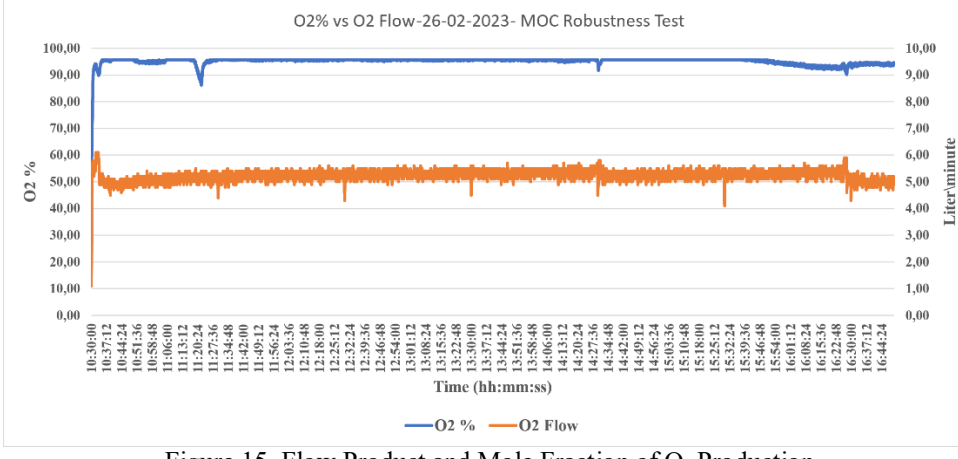

Figure 15. Flow Product and Mole Fraction of O_2 Production

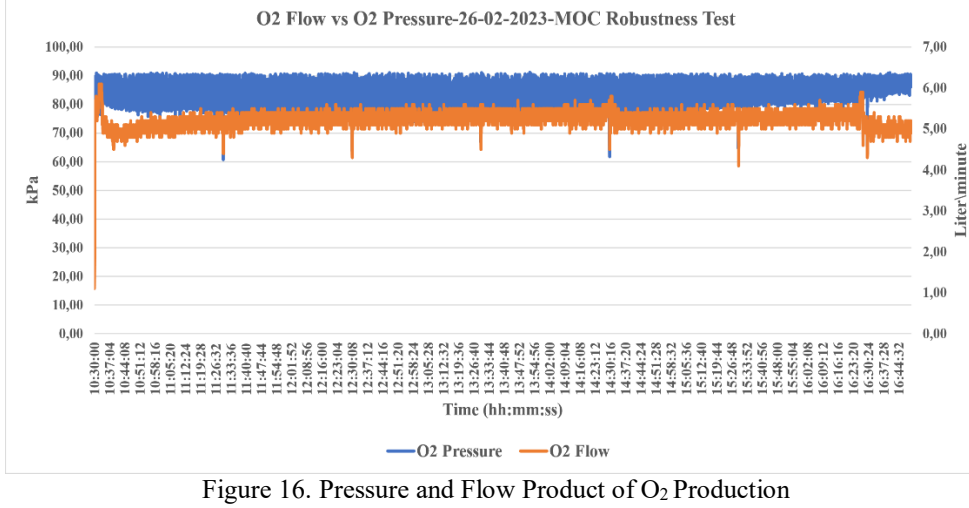

Figure 16. Pressure and Flow Product of O_2 Production

7. Conclusions

In this work, the adsorption cycle time of the zeolite must be taken into consideration while using the PSA method to develop an oxygen concentrator (Oxycon) that can produce approximately 95% pure oxygen. There is an appropriate cycle time so that N2 adsorption and O2 release by zeolite are optimal. Oxycon, with a production capacity of 5 Lpm and a production capacity of 10 Lpm, has different PSA cycle times to produce oxygen. An oxygen concentrator with a production capacity of 5 Lpm requires a gas supply with a pressure of at least 200kPa, which is flowed into the adsorption zeolite tube. The dimensions of the adsorption tube, which contains zeolite, also have an influence on the duration of the saturation time of N2 gas adsorption. Based on the experimental results, the configuration of the valve open and close system timer in the Oxycon implementation gives optimal results in the time cycle 2 (S2), has a time duration of Pressurization and Adsorption (PR & AD) of 4000 milliseconds, blow down (BD) 350 milliseconds, blow down and equalization (BD & EQ) 650 milliseconds, purge (PG) 4000 milliseconds, equalization (EQ) 350 milliseconds, and pressurization (PR) 650 milliseconds. By finding the optimal gate valve open/close timing, pure oxygen production can be fulfilled for the patient's oxygen therapy needs. At the same time, the O2 gas pressure collected in the collector tube has a stable pressure at a value of 80-90 kPa for an O2 gas flow rate of 4-5 Lpm. In addition to the timer parameter in the algorithm in the proposed MOC design, it is also necessary to pay attention to several other parameters; therefore, the goal of making MOC with the PSA method to produce 95% pure oxygen stably can be achieved. Other parameters in question are the design and implementation of zeolite sieve adsorber tubes, the design and implementation of moisture reduction in water removal and moisture removal, and the design and implementation of pressure stabilizers supplied from compressor pumps. In future work, it is very important to conduct research related to optimizing the reduction of air humidity to below 50% to reduce excess air humidity, which causes the quality of the zeolite sieve to decline rapidly. By implementing the Internet of Things and machine learning, future research can be carried out by monitoring and predicting the performance of the zeolite sieve; therefore, the MOC performance can be maintained so that it can produce >95% pure oxygen stably safely and sustainably.

8. References

[1]. M. W. Ackley, *Medical oxygen concentrators: a review of progress in air separation technology*, vol. 25, no. 8. Springer US, 2019.

[2]. M. Meena *et al.*, "Home-based long-term oxygen therapy and oxygen conservation devices: An updated review," *Natl. J. Physiol. Pharm. Pharmacol.*, vol. 5, no. 4, pp. 267–274, 2015, doi: 10.5455/njppp.2015.5.0912201429.

[3]. G. Hardavella, I. Karampinis, A. Frille, K. Sreter, and I. Rousalova, "Oxygen devices and delivery systems," *Breathe*, vol. 15, no. 3, pp. e108–e116, 2019, doi: 10.1183/20734735.0204-2019.

[4]. D. C. Martin, "Contemporary portable oxygen concentrators and diverse breathing behaviours-A bench comparison," *BMC Pulm. Med.*, vol. 19, no. 1, pp. 1–11, 2019, doi: 10.1186/s12890-019-0980-x.

[5]. K. Ogawa, Y. Inagaki, and A. Ohno, "Numerical analysis of O2 concentration, gas-zeolite temperatures in two zeolite columns for an oxygen concentrator," *Int. J. Heat Mass Transf.*, vol. 129, pp. 238–254, 2019, doi: 10.1016/j.ijheatmasstransfer.2018.09.052.

[6]. Q. Zhang *et al.*, "Experimental study on oxygen concentrator with wide product flow rate range: individual parametric effect and process improvement strategy," *Sep. Purif. Technol.*, vol. 274, no. May, p. 118918, 2021, doi: 10.1016/j.seppur.2021.118918.

[7]. H. Aljaghoub, S. Alasad, A. Alashkar, M. Almallahi, and R. Hasan, "Comparative analysis of various oxygen production techniques using multi-criteria decision-making methods," *Int. J. Thermofluids*, vol. 17, no. December 2022, p. 100261, 2023, doi: 10.1016/j.ijft.2022.100261.

[8]. Z. Qiao, Z. Wang, C. Zhang, S. Yuan, Y. Zhu, and J. Wang, "PVAm–PIP/PS composite membrane with high performance for CO_2/N_2 separation," *AIChE J.*, vol. 59, no. 4, pp. 215–228, 2012, doi: 10.1002/aic.

[9]. S. W. Chai, M. V. Kothare, and S. Sircar, "Rapid pressure swing adsorption for reduction of bed size factor of a medical oxygen concentrator," *Ind. Eng. Chem. Res.*, vol. 50, no. 14, pp. 8703–8710, 2011, doi: 10.1021/ie2005093.

[10]. M. D. Urich, R. R. Vemula, and M. V Kothare, "Implementation of an embedded model predictive controller for a novel medical oxygen concentrator R," *Comput. Chem. Eng.*, vol. 160, p. 107706, 2022, doi: 10.1016/j.compchemeng.2022.107706.

[11]. R. Slade and A. Bauen, "Micro-algae cultivation for biofuels: Cost, energy balance, environmental impacts and future prospects," *Biomass and Bioenergy*, vol. 53, no. 0, pp. 29–38, 2013, doi: 10.1016/j.biombioe.2012.12.019.

[12]. S. Tesch, T. Morosuk, and G. Tsatsaronis, "Comparative evaluation of cryogenic air separation units from the exergetic and economic points of view," *Low-temperature Technol.*, vol. 30, p. 159, 2019.

[13]. M. J. Hauser, "Cost evaluation and life cycle assessment of biogas upgrading technologies for an anaerobic digestion case study in the United States," NTNU, 2017.

[14]. I. A. Flameling and J. Kromkamp, "Light dependence of quantum yields for PSII charge separation and oxygen evolution in eucaryotic algae," *Limnol. Oceanogr.*, vol. 43, no. 2, pp. 284–297, 1998, doi: 10.4319/lo.1998.43.2.0284.

[15]. M. A. Fahim, T. A. Alsahhaf, and A. Elkilani, "Chapter 11 - Hydrogen Production," in *Fundamentals of Petroleum Refining*, M. A. Fahim, T. A. Alsahhaf, and A. Elkilani, Eds. Amsterdam: Elsevier, 2010, pp. 285–302.

[16]. A. F. Clarens, E. P. Resurreccion, M. A. White, and L. M. Colosi, "Environmental Life Cycle Comparison of Algae to Other Bioenergy Feedstocks," *Environ. Sci. Technol.*, vol. 44, no. 5, pp. 1813–1819, Mar. 2010, doi: 10.1021/es902838n.

[17]. Q. Sun, H. Li, J. Yan, L. Liu, Z. Yu, and X. Yu, "Selection of appropriate biogas upgrading technology-a review of biogas cleaning, upgrading and utilisation," *Renew. Sustain. Energy Rev.*, vol. 51, pp. 521–532, 2015, doi: https://doi.org/10.1016/j.rser.2015.06.029.

[18]. M. HERR, A. LERMEN, and S. ROSTEK, "Biogasgrid Injection in Germany and Europe-Market, Technology and Players," *Berlin Dtsch. Energ. Agent. GmbH*, 2010.

[19]. "Membrane separation technology market by application & region - global forecast 2022," 2023. https://www.marketsandmarkets.com/Market-Reports/membrane-separation-technology-market-267308161.html.

[20]. R. V Piloni, I. C. Daga, C. Urcelay, and E. L. Moyano, "Experimental investigation on fast pyrolysis of freshwater algae. Prospects for alternative bio-fuel production," *Algal Res.*, vol. 54, p. 102206, 2021, doi: https://doi.org/10.1016/j.algal.2021.102206.

[21]. P. Rao and M. Muller, "Industrial oxygen: its generation and use," in *ACEEE summer study on energy efficiency in industry*, 2007, vol. 6, pp. 124–135.

[22]. J. C. Santos, P. Cruz, T. Regala, F. D. Magalhães, and A. Mendes, "High-Purity Oxygen Production by Pressure Swing Adsorption," *Ind. Eng. Chem. Res.*, vol. 46, no. 2, pp. 591–599, Jan. 2007, doi: 10.1021/ie060400g.

[23]. D. Ariono and A. K. Wardani, "Review of Membrane Oxygen Enrichment for Efficient Combustion," *J. Phys. Conf. Ser.*, vol. 877, no. 1, pp. 0–7, 2017, doi: 10.1088/1742-6596/877/1/012050.

[24]. K. Ogawa, Y. Inagaki, and A. Ohno, "Numerical analysis of O 2 concentration , gas-zeolite temperatures in two zeolite columns for an oxygen concentrator," *Int. J. Heat Mass Transf.*, vol. 129, pp. 238–254, 2019, doi: 10.1016/j.ijheatmasstransfer.2018.09.052.
[25]. L. Moroney, "The Firebase Realtime Database," *Defin. Guid. to Firebase*, pp. 51–71, 2017, doi: 10.1007/978-1-4842-2943-9_3.
[26]. A. Dennis, Barbara H. Wixom, and R. M. Roth, *System Analysis and Design 5th Edition*. John Wiley & Sons, Inc., 2012.
[27]. N. A. I. Hasanah, D. Maryetnowati, F. N. Edelweis, F. Indriyani, and Q. Nugrahayu, "The climate comfort assessment for tourism purposes in Borobudur Temple Indonesia," *Heliyon*, vol. 6, no. 12, p. e05828, 2020, doi: 10.1016/j.heliyon.2020.e05828.
[28]. E. Husni *et al.*, "Microclimate investigation of vehicular traffic on the urban heat island through IoT-Based device," *Heliyon*, vol. 8, no. 11, p. e11739, 2022, doi: 10.1016/j.heliyon.2022.e11739.
[29]. F. Yang, J. Wu, X. Zhu, T. Ge, and R. Wang, "Enhanced stability and hydrophobicity of LiX@ZIF-8 composite synthesized environmental friendly for CO2 capture in highly humid flue gas," *Chem. Eng. J.*, vol. 410, no. October 2020, p. 128322, 2021, doi: 10.1016/j.cej.2020.128322.
[30]. M. Santoso *et al.*, "Long term characteristics of atmospheric particulate matter and compositions in Jakarta, Indonesia," *Atmos. Pollut. Res.*, vol. 11, no. 12, pp. 2215–2225, 2020, doi: 10.1016/j.apr.2020.09.006.
[31]. Mospec, "Plastic Medium-Power Complemtary Silico Transistor."
[32]. A. P. Malvino, *Electronic principles / Albert Paul Malvino*. McGraw-Hill New York, 1973.

Galang Adira Prayoga received the bachelor's degree in physics from Diponegoro University Semarang, in 2020. He does research in the field of machine learning to detect broken solar cells with clustering heat distribution using thermograph camera. Master's degree in electrical engineering from Institut Teknologi Bandung. He is currently working as a researcher with Institut Teknologi Bandung. His research interests are the embedded system, Internet of things, and machine learning.

Emir Husni received the Ir. degree in electrical engineering from Institut Teknologi Bandung, in 1992, and the M.Sc. degree in satellite technology and the Ph.D. degree in satellite communication from the University of Surrey, U.K., in 1994 and 1997, respectively. He is currently a Professor with the School of Electrical Engineering and Informatics, Institut Teknologi Bandung. His research interests are intelligent transportation systems, satellite technology, and the Internet of Things.

Salahudin Damar Jaya received the Drs. degree in faculty science and mathematics Institut Teknologi Bandung, in 1992. He is currently working as a scientist and professional in an enterprise developing medical device mobile.